Iranian Journal of Materials Science and Engineering, Vol. 19, Number 2, June 2022
RESEARCH PAPER

In Vitro Release Kinetics of Curcumin from Thermosensetive Gelatin-Chitosan Hydrogels Containing Zinc Oxide Nanoparticles

Shadi Moshayedi, Hossein Sarpoolaky, Alireza Khavandi

* *hsarpoolaky@iust.ac.ir*

School of Materials and Metallurgical Engineering, Iran University of Science and Technology, Tehran, Iran

Received: January 2022 **Revised: March 2022** **Accepted: April 2022**

DOI: 10.22068/ijmse.2633

Abstract: *In this paper, chemically-crosslinked gelatin/chitosan hydrogels containing zinc oxide nanoparticles (ZNPs) were loaded with curcumin (CUR) and their microstructural features, physical properties, the drug entrapment efficiency, and curcumin release kinetics were evaluated using scanning electron microscopy (SEM), the liquid displacement method, and UV–Vis spectroscopy. The in vitro kinetics of drug release was also studied using the First-order, Korsmeyer-Peppas, Hixon-Crowell, and Higuchi kinetic models. The SEM micrographs confirmed the formation of highly porous structures possessing well-defined, interconnected pore geometries. A significant reduction in the average pore size of the drug-loaded hydrogels was observed with the addition of ZNPs and CUR to the bare hydrogels. A high value of drug loading efficiency (~ 72 %) and a maximum curcumin release of about 50 % were obtained for the drug-loaded specimens. It was found that curcumin was transported via the non-Fickian diffusion mechanism. The kinetics of drug release was best described by the Hixon-Crowell, Higuchi, and Korsmeyer-Peppas models, demonstrating that curcumin release was controlled by the diffusion of drug molecules and the degradation and swelling of the drug carrier. However, a lower degree of fitting was observed with the First-order kinetic model.*

Keywords: *gelatin, chitosan, zinc oxide, curcumin, release kinetics.*

1. INTRODUCTION

Curcumin is a non-toxic active compound derived from the rhizome of *Curcuma longa* plant that exhibits a wide range of therapeutic activities like anti-inflammatory, anti-tumor, antioxidant, anti-cancer, etc. [1]. However, its low bioavailability, low hydrophilicity, physicochemical instability, and short half-life have restricted its clinical effects [2]. To overcome these limitations, curcumin can be encapsulated within a proper drug carrier, such as a polymeric scaffold like hydrogels. As a brief introduction, hydrogels are three-dimensional (3D) networks capable of holding large amounts of water within their porous structures while resisting hydrolytic degradation. Due to their high porosity, high hydrophilicity, and excellent swelling behavior, hydrogels have been found numerous applications in the field of tissue engineering, drug delivery, agriculture, etc. [3]. Until now, these materials have been made from various synthetic or natural compounds such as polyvinyl alcohol (PVA), polyvinylpyrrolidone (PVP), collagen, gelatin, chitosan, etc. [4]. Gelatin is one of the best-known, widely used proteins, which is obtained from the partial acid or alkaline hydrolysis of fibrous collagen. Properties such as low cost, non-toxicity, biodegradability, and high-water absorption have suggested gelatin as an excellent candidate for biomedical applications [5]. However, the application of pure gelatin hydrogels has been limited due to their high degree of water solubility, low thermal stability, and poor strength [6]. Chitosan is another well-known polymer derived from N-deacetylation of chitin, which has been widely used to overcome the inherent limitations of pure gelatin [7]. Due to its high availability, high biocompatibility, biodegradability, and non-antigenicity, chitosan has been proposed for a wide range of applications, including the fabrication of tissue engineering scaffolds [8], drug carriers [9], films for food preservation, [10] etc. Despite the excellent properties that the addition of chitosan to gelatin hydrogels are responsible for, the combination of these two biopolymers still lacks sufficient mechanical strength and hydrolytic resistivity [11], which can be improved by the formation of covalent bonds between the functional groups of polymer chains and a proper crosslinking agent such as genipin [12]. In recent years, nanocomposite hydrogels, a mixture of multi phases one of which has at least one

[DOI: 10.22068/ijmse.2633]

dimension less than 100 nm, have been introduced to enhance the stability, strength, or drug loading/unloading efficacy of the polymeric hydrogels. Zinc oxide nanoparticles are amongst the proposed compounds, which have been received growing attention [13, 14] due to their unique therapeutic activities such as antibacterial, antimicrobial, anti-inflammatory, anti-diabetic, and anti-cancer properties [15]. These unique properties encouraged us to study the addition of zinc oxide nanoparticles to gelatin/chitosan blends *in situ*-loaded with curcumin. To the best of our knowledge, the combination of these compounds is not yet known, which can be proposed as a potential drug carrier. Further, the literature survey has indicated that the kinetics of drug release is an important characteristic of a drug loading system, which can provide valuable information on the concentration of the drug in plasma and also determine the mechanism by which the drug release process is mainly controlled that seems to be a helpful tool for the control and optimization of drug release. Considering the importance of drug release kinetics, no one as far as we know has conducted a systematic study on the transport mechanism of curcumin and its release kinetics from the gelatin/chitosan/zinc oxide nanocomposites, which were assessed deeply in the current study.
In this paper, we proposed genipin-crosslinked gelatin/ chitosan/ zinc oxide nanocomposite hydrogels as a novel carrier for the controlled delivery of curcumin. In this context, curcumin-loaded hydrogels were first prepared *via* the polymer casting method in combination with lyophilization. The microstructural features, porosity, and drug loading capacity of the prepared hydrogels were evaluated using SEM, the liquid displacement method and UV-Vis spectroscopy. Further, the kinetic models, which best describe curcumin release from the drug-loaded hydrogels were also studied and discussed in detail.

2. EXPERIMENTAL PROCEDURE

2.1. Materials

Chitosan (C, Medium molecular weight, degree of deacetylation ~ 75-85 %), Gelatin (G, derived from pigskin), Genipin (GP, > 98 %), and zinc oxide nanoparticles (ZNPs, 50-100 nm) were purchased from Sigma Aldrich (Germany), Merck Millipore (Germany), China, and Armina Co. (Iran), respectively. Curcumin (CUR) was obtained from ExirNanoSina Co. (Iran). Phosphate buffered saline tablets (PBS) with 10 X concentration were supplied from Zist Mavad Pharmed (Iran). All other solvents and reagents were of analytical grade and used as received without further purification.

2.2. Fabrication of drug-loaded nanocomposite hydrogels

Curcumin (40 mg) was first solubilized in 1 % acetic acid solution. Chitosan was then added to a certain amount of the above solution to keep the primary concentration of the drug at 2.5 % w/w relative to the total polymer content. Afterwards, an aqueous solution of gelatin was prepared by dissolving gelatin in 1% acetic acid solution at 30-35°C and was added to the chitosan solution with the gelatin to chitosan weight ratio of 3:2 and final solid concentration of 4% w/v. This step was followed by adding ZNPs and GP solution (both with the concentration of 1.5% w/w) to the prepared homogenous solution. Next, the blends were cast into polypropylene cylindrical molds (Ø9 mm) to approximately 4- 5 mm height and kept at room temperature for 18 h. The crosslinked hydrogels were then frozen at -20 and -65°C for a minimum of 48 h and lyophilized for 24 h (FD-10, Pishtaz Engineering Company, Iran). It is worth noting that throughout this paper, gelatin/ chitosan and curcumin-loaded gelatin/ chitosan/ ZNPs hydrogels are called GC, GCZ, and *CUR-GCZ*, respectively, as shown in Table 1.

Table 1. Sample codes

Sample codes	G:C (w/w)	GP (%w/w)	ZnO (%w/w)	CUR (%w/w)
GC	3:2	1.5	0	0
CUR-GCZ	3:2	1.5	1.5	2.5

2.3. Characterization

2.3.1. Porosity measurement

The porosity of the nanocomposite hydrogels was determined using the liquid displacement method. In brief, the lyophilized specimens were cut into cylinders and immersed in anhydrous ethanol until was saturation achieved. The porosity was then determined using the following equation [16]:

$$P\ (\%) = (W_2\text{-}W_1\text{-}W_3)/(W_2\text{-}W_3) \times 100 \qquad (1)$$

[DOI: 10.22068/ijmse.2633]

where W_1 indicates the initial dry weight of the samples (g). W_2 represents the weight of the container, ethanol, and the saturated hydrogel (g). W_3 denotes the weight of the container and the remained ethanol after the removal of the saturated hydrogel (g).

2.3.2. Morphological observation

In order to examine the microstructure of the drug-loaded hydrogels, TESCAN Vega II scanning electron microscope (Czech) was used at an accelerating voltage of 20 kV. Prior to the evaluation, the lyophilized specimens were fractured and gold-coated to avoid the surface charge build-up. The average size of the pores was also measured using ImageJ software by the random selection of at least 100 different pores in each group of hydrogels.

2.3.3. Drug encapsulation efficiency

The nanocomposite hydrogels were added to screw-cap centrifuge tubes that contained 10 ml ethanol, followed by incubation at 37°C. After removing the specimens at predetermined time intervals, the absorption of the solutions was measured at 424 nm on a UV-Vis spectrophotometer (UV-2559, Shimadzu, Japan) to determine the real CUR contents. The above steps were repeated until CUR could not be detected. Drug encapsulation efficiency (EE) was then calculated using the equation as follows [17]:

$$EE\ (\%) = M_{real}/M_{th} \times 100 \quad (2)$$

where M_{real} and M_{th} indicate the real and theoretical concentrations of curcumin in the drug-loaded hydrogels, respectively.

2.3.4. In vitro drug release

The release behavior of CUR from the drug-loaded nanocomposite hydrogels was determined in PBS solution (pH= 7.4) at room temperature and 37°C.

To this end, a specific amount of hydrogels (20-30 mg) were soaked in 10 ml of PBS at the temperatures mentioned above. Afterward and at prearranged time points, the specimens were taken out from the vials, and the absorbance of the yellow solutions was recorded on a UV-Visible spectrophotometer (UV-2559, Shimadzu, Japan) at 424 nm. The CUR contents were determined using the standard calibration equation, and the accumulative release percentage was calculated using the equation below [17, 18]:

$$\text{CUR cumulative release } (\%) = M_t/M_0 \times 100 \quad (3)$$

where M_t and M_0 denote the amount of CUR released at time t and the total content of the drug encapsulated in the hydrogels, respectively.

2.3.5. Drug Release kinetics

To examine the kinetics and mechanism of *in vitro* CUR release from the drug-loaded nanocomposite hydrogels, various mathematical models were utilized, including the Korsmeyer-Peppas, First-order, Hixson-Crowell, and Higuchi models, which are introduced by the following equations [17, 19]:

$$\text{Korsmeyer-Peppas: } M_t/M_\infty = kt^n \quad (4)$$

where M_t and M_∞ represent the amount of CUR released at time t and the equilibrium state ($t= \infty$), respectively, k denotes the release constant, indicating the drug release rate, and n is known as the release exponent that identifies the drug release mechanism. It is crucial to note that the Korsmeyer-Peppas model is only applied where $M_t/M_\infty \leq 0.6$ [17, 20].

First-order kinetic model:

$$\text{Ln } [M_\infty/(M_\infty - M_t)] = kt \quad (5)$$

$$\text{Hixson-Crowell model: } (1 - M_t/M_\infty)^{1/3} = -kt \quad (6)$$

$$\text{Higuchi model: } M_t/M_\infty = kt^{1/2} \quad (7)$$

In this paper, correlation coefficients, R^2, equal to or higher than 0,98 were considered acceptable.

2.3.6. Statistical analysis

All data were expressed as the mean ± standard deviation (SD). Statistical analysis was carried out using one-way analysis of variance (ANOVA). A probability value of 95% ($P < 0.05$) was considered to be statistically significant.

3. RESULTS AND DISCUSSION

3.1. Porosity

Fig. 1 compares the porosity values of GC and CUR-GCZ hydrogels, which were calculated using the liquid displacement method.

As can be seen in this figure, all specimens displayed high porosity values greater than 88 %, demonstrating the formation of interconnected pore spaces, which will ensure high water absorption and thus enhanced drug release behavior. Further, it is apparent from Fig. 1 that the porosity of hydrogels decreased markedly upon the simultaneous addition of ZNPs and CUR, but none of these differences were statistically significant ($P >0.05$), which seem to

[DOI: 10.22068/ijmse.2633]

imply that the porosity of gelatin/chitosan hydrogels is independent of the added ZNPs and CUR. However, the reason for this unexpected result can be attributed to the second role of curcumin molecules as the crosslinking agent in the discussed system. Further tests will need to be undertaken to confirm this hypothesis.

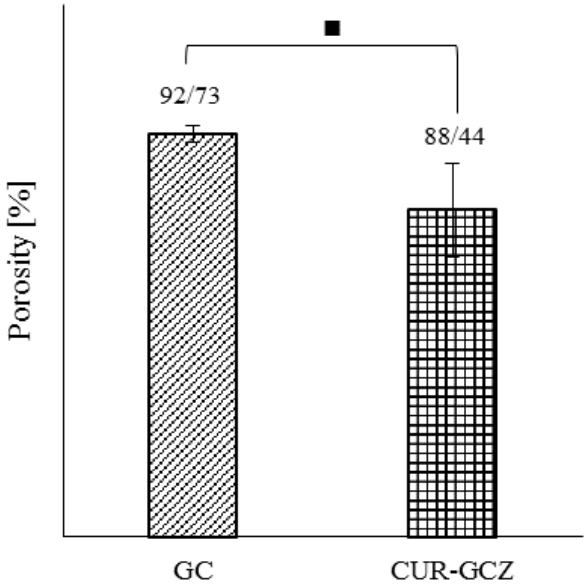

Fig. 1. Comparison of the porosity values of GC and CUR-GCZ hydrogels calculated using the liquid displacement method (■: P >0.05)

3.2. Microstructure

The cross-sectional micrographs of GC and CUR-GCZ hydrogels and corresponding pore size distributions are depicted in Fig. 2, which reveal the formation of highly porous specimens with well-defined, interconnected macropores that are believed to favor the transport of nutrients to and metabolic wastes from the cells, exchange of gases, swelling capacity, and release of the loaded drug from CUR-GCZ hydrogels. Additionally, as can be seen in this figure, the drug-loaded hydrogels possessed a finer microstructure compared with the bare gelatin/chitosan hydrogels (50 to 200 µm for CUR-GCZ vs. 100 to 300 µm for GC specimens). The reduction in the average pore sizes of the drug-loaded nanocomposite hydrogels appears to slow down the water absorption process and subsequent drug release behavior. This correlates reasonably well with Varghese [21]. The finer microstructure of curcumin-loaded nanocomposite hydrogels is further indicated in Fig. 3.

There are several possible explanations for this outcome, which can be first explained by the higher viscosity of CUR-GCZ hydrogels in comparison with that of GC specimens that is believed to prevent further growth of ice crystals during the solidification step [22]. Another possible reason for this can be related to the presence of a second phase in the polymeric system (herein, CUR and ZNPs) that has occupied part of the hydrogels' pore spaces as proposed previously by Ghaee [23].

3.3. Encapsulation efficiency and *in vitro* release behavior

To explore the ability of the nanocomposite hydrogels to accommodate hydrophobic drugs like curcumin, 2.5% w/w curcumin nanomicelles were added to the primary solution of polymers before gelation occurred. Then, using equation 2, the encapsulation efficiency of 72.31 ± 1.96 % was obtained for the curcumin-loaded gelatin/ chitosan/ ZNPs hydrogels, exhibiting the good loading ability and proper choice of the encapsulation strategy.

Fig. 4 illustrates the accumulative release percentage of CUR from the CUR-GCZ hydrogels in PBS at room temperature and 37°C, which indicates a burst release during the first six hours of the experiment, followed by a sustained release over the next 18 h. The initial rapid release of CUR can be attributed to the enhanced solubility of CUR nanomicelles and the removal of the drug from the surfaces of the CUR-loaded GCZ hydrogels [24].

Additionally, we noted that the prepared drug-loaded nanocomposites showed much higher drug release rates compared with the previous findings in the literature. More precisely, herein, 21 and 36% of CUR were released at room temperature and 37°C, respectively in the first six hours of the experiment, which were much higher than the values reported by Nguyan [25], Hu [26], and Chen [17]. The enhancement of CUR release may have occurred due to the higher porosity values of the as-prepared hydrogels.

3.4. Drug release kinetics

As was stated in the *Experimental Procedure*, five different mathematical models were employed to explore kinetics of drug release from the CUR-loaded GCZ hydrogels.

[DOI: 10.22068/ijmse.2633]

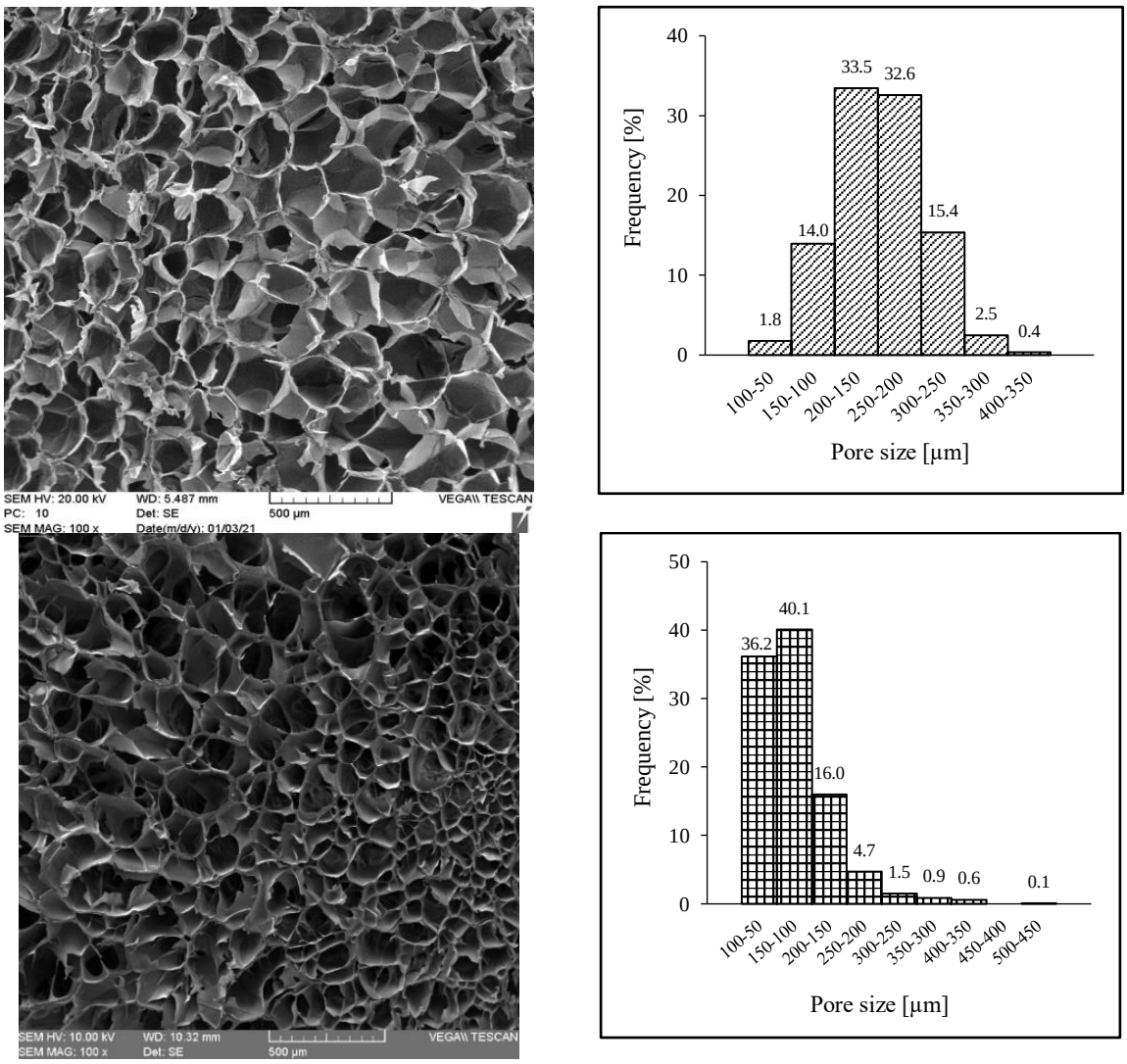

Fig. 2. SEM micrographs of: (a) GC and (b) CUR-GCZ hydrogels, indicating the formation of highly porous microstructures with well-defined, interconnected pore spaces.

The *in vitro* kinetic parameters that were extracted from the graphs depicted below for each kinetic model together with their correlation coefficients (R^2) are listed in Table 1. It is worthwhile noting that the best fitted mathematical model is considered to be the one that provides R^2 values closest to one.

In vitro drug release data were first approximated with the Korsmeyer-Peppas model (Fig. 5), which is a semi-empirical model, providing valuable information on the mechanism of drug release from the CUR-GCZ hydrogels. As can be seen, the values of R^2 were greater than 0.986 at both temperatures, demonstrating that the kinetics of CUR release can be described using Korsmeyer-Peppas model.

It should be mentioned that the release exponent of the Korsmeyer-Peppas model, n, can adopt various values depending on the geometry of the drug-loaded carrier. For cylindrical hydrogels, which was the case of the current study, n values smaller than 0.45 indicate a *Fickian diffusion* mechanism; n values between 0.45 to 0.89 show a *non-Fickian transport* behavior; and the values equal to or higher than 0.89 demonstrate *Case II transport* (zero-order) [20].

In the present study, n was approximately 0.67, indicating that drug release was controlled by a non-Fickian transport. In other words, the drug release kinetics was controlled by both diffusion and polymer chains relaxation and thus, for the current system, factors that affect the drug diffusion (such as the temperature, diffusion

[DOI: 10.22068/ijmse.2633]

length, crystallization degree of the carrier, agitation etc.) can be regulated to control the rate of drug release from the CUR-GCZ hydrogels.

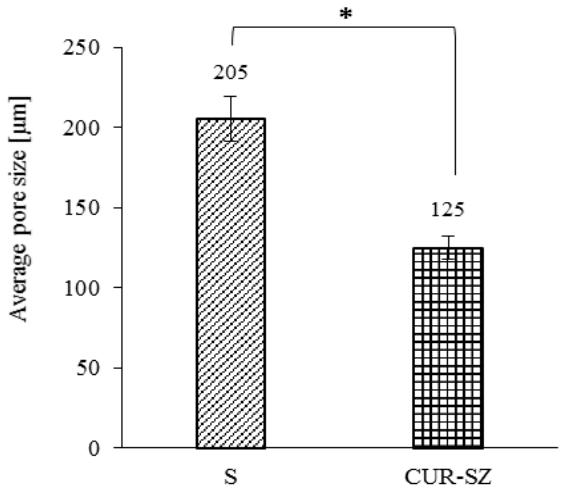

Fig. 3. Average pore sizes of GC and CUR-GCZ nanocomposite hydrogels (*: P< 0.05)

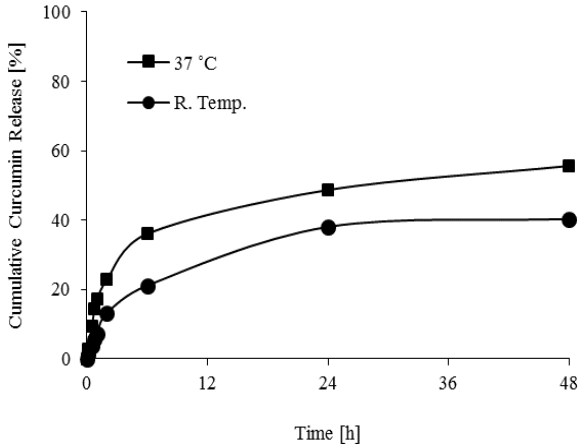

Fig. 4. Dependency of the in vitro release profiles of CUR to the temperature, indicating the thermo-responsive nature of the prepared hydrogels

Fig. 6 shows that the *in vitro* experimental release data and predicted values obtained from the First-order kinetic model were fitted to the lower degree ($R^2 \sim 0.963$). This would appear to suggest that the CUR release rate may not be merely dependent on the drug concentration. The CUR release data were also modeled using the Hixson-Crowell model (Fig. 7). As can be seen, there is a strong correlation between the experimental and predicted values ($R^2 > 0.982$), demonstrating that CUR release was controlled by the erosion, dissolution, and degradation behavior of the hydrogels.

The results of the approximations of the curcumin release data to the Higuchi model are shown in Fig. 8. From this figure, we can see that the kinetics of CUR release at room temperature perfectly followed the Higuchi model ($R^2 \sim 0.988$), suggesting that release kinetics was dependent on both the swelling and degradation behavior of the prepared hydrogels and so, the test temperature and time can be modulated to control the rate of curcumin release from CUR-GCZ hydrogels.

Contrary to the results obtained at room temperatures, insufficient fitting was observed at 37°C ($R^2 \sim 0.925$), although this proximity was enhanced for the first six hours of the experiment ($R^2 \sim 0.986$).

4. CONCLUSIONS

In this paper, a strategy was planned to encapsulate 2.5 % curcumin in gelatin/ chitosan/ ZNPs nanocomposite hydrogels *in situ via* the solution casting method followed by lyophilization.

The drug-loaded hydrogels indicated high porosity values and well-defined interconnected pore spaces which would enhance the swelling rate, water absorption capacity, and consequently, drug release characteristics of the prepared specimens. Furthermore, these hydrogels demonstrated high encapsulation efficiency of 72% and a thermo-sensitive drug release behavior. This could potentially can lead to both wound dressing applications and *in vivo* drug delivery systems. Additionally, the curcumin release profiles showed a high initial burst release, greater than the values reported previously in the literature, that guarantees the rapid release of chemically unstable drugs such as curcumin. Finally, our findings showed that kinetics of drug release was best described by the Hixon-Crowell model and thus, was mainly controlled by *in vitro* degradation of the drug-loaded hydrogels.

ACKNOWLEDGEMENTS

This work was supported by Iran University of Science and Technology. We would like to acknowledge the *Central Reference Laboratory* of Iran University of Science and Technology and the *Advance Materials Laboratory* of Amirkabir University of Technology for their ongoing cooperation in our experimental work.

[DOI: 10.22068/ijmse.2633]

Table 2. In vitro kinetic parameters extracted from the Korsmeyer-Peppas, First-order, Hixon-Crowell, and Higuchi kinetic models, which were used to describe the release behavior of curcumin from the CUR-GCZ hydrogels at room temperature and 37°C.

	Room Temperature		37 ˚C	
CUR-GCZ	k (g/g.min)	R^2	k (g/g.min)	R^2
Korsmeyer-Peppas	0.0112	0.9863	0.0203	0.9888
First-order	0.0022	0.9629	0.0036	0.9637
Hixson-Crowell	0.0007	0.9971	0.0007	0.9818
Higuchi	0.0274	0.9884	0.0404	0.9864

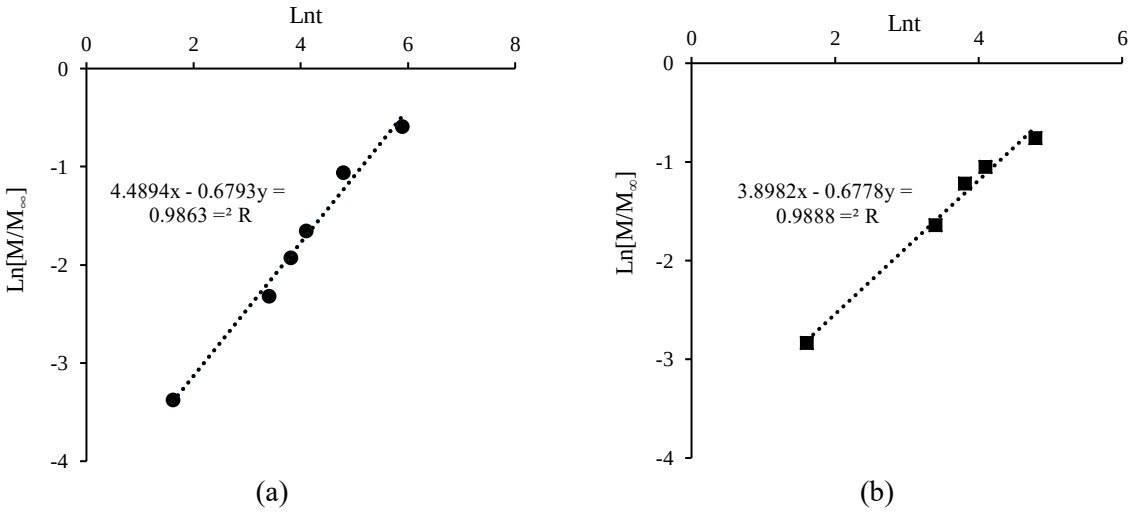

Fig. 5. In vitro curcumin release data modelled using the Korsmeyer-Peppas kinetic model at: (a) room temperature and (b) 37°C

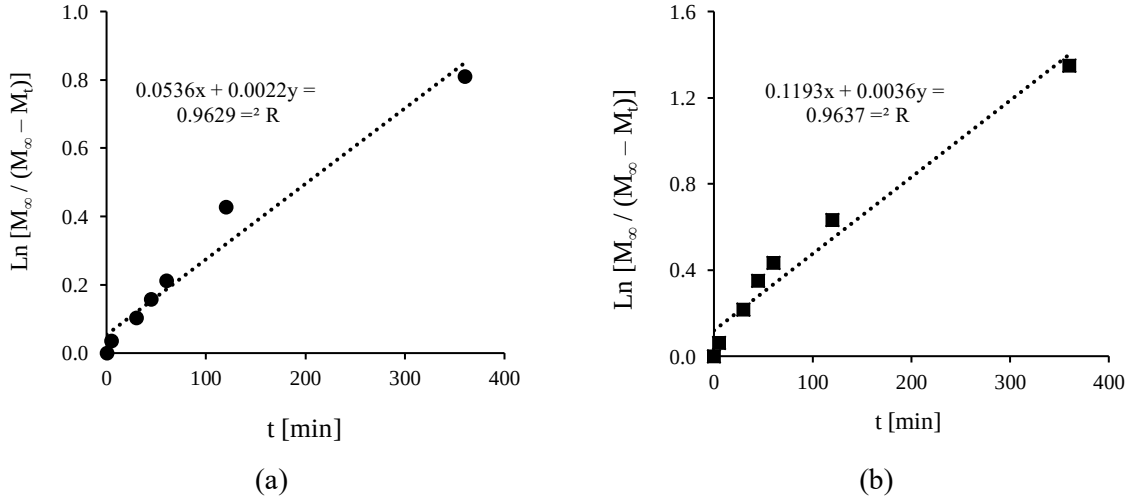

Fig. 6. Approximations of the in vitro curcumin release data to the First-order kinetic model at: (a) room temperature and (b) 37°C after six hours

[DOI: 10.22068/ijmse.2633]

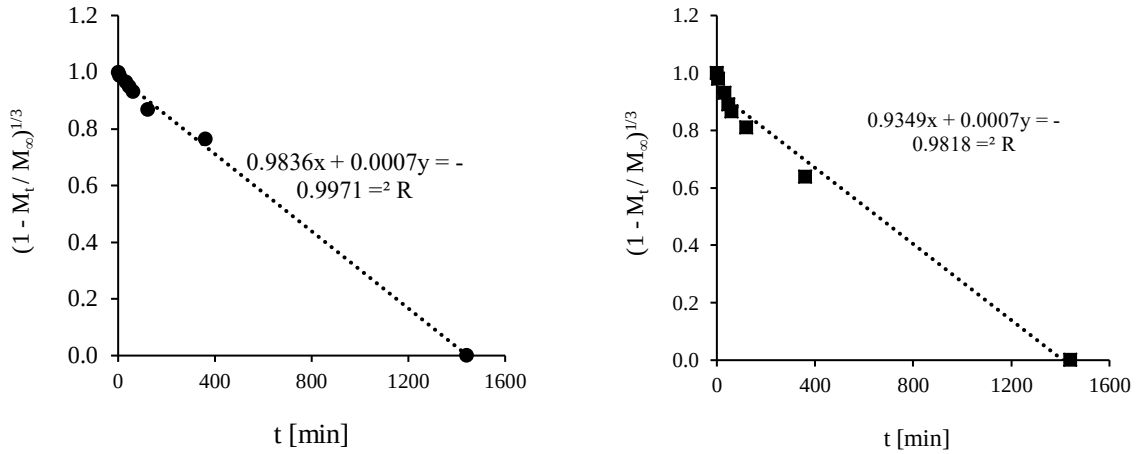

Fig. 7. In vitro drug release data approximated using the Hixon-Crowell model at: (a) room temperature and (b) 37°C

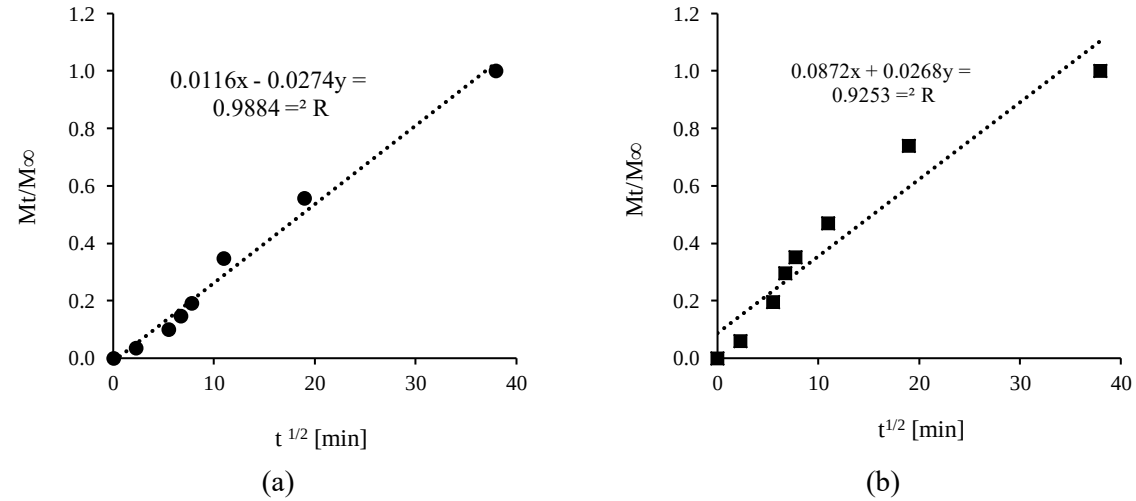

Fig. 8. Approximations of the in vitro curcumin release data to the Higuchi model at: (a) room temperature and (b) 37°C

REFERENCES

[1] Joe, B., Vijaykumar, M. and Lokesh, B. R., "Biological Properties of Curcumin-Cellular and Molecular Mechanisms of Action." Crit Rev Food Sci Nutr, 2004, 44, 97-111.

[2] Her, C., Venier-Julienne, M.-C. and Roger, E., "Improvement of Curcumin Bioavailability for Medical Applications." Medicinal Aromat. Plants, 2018, 07, 1-15.

[3] El-Sherbiny, I. M. and Yacoub, M. H., "Hydrogel Scaffolds for Tissue Engineering: Progress and Challenges." Glob. cardiol. sci. pract., 2013, 2013, 316-342.

[4] Chhibber, T., Shinde, R., Lahooti, B., Bagchi, S., Varahachalam, S., Gaddam, A., Jaiswal, A., Gracia, E., Chand, H., Kaushik, A. and Jayant, R., Hydrogels in Tissue Engineering, Intelligent Hydrogels in Diagnostics and Therapeutics, ed. A. Ghosal and A. Kaushik, Boca Raton, USA, 2020. 105-122.

[5] Nie, L., Wu, Q., Long, H., Hu, K., Li, P., Wang, C., Sun, M., Dong, J., Wei, X., Suo, J., Hua, D., Liu, S., Yuan, H. and Yang, S., "Development of Chitosan/Gelatin Hydrogels Incorporation of Biphasic Calcium Phosphate Nanoparticles for Bone Tissue Engineering." J. Biomater. Sci. Polym. Ed., 2019, 30, 1636-1657.

[6] Bello, A. B., Kim, D., Kim, D., Park, H.

[DOI: 10.22068/ijmse.2633]

and Lee, S. H., "Engineering and Functionalization of Gelatin Biomaterials: From Cell Culture to Medical Applications." Tissue Eng Part B Rev, 2020, 26, 164-180.

[7] Li, H., Hu, C., Yu, H. and Chen, C., "Chitosan Composite Scaffolds for Articular Cartilage Defect Repair: A Review." RSC Advances, 2018, 8, 3736-3749.

[8] Dimida, S., Barca, A., Cancelli, N., De Benedictis, V., Raucci, M. G. and Demitri, C., "Effects of Genipin Concentration on Cross-Linked Chitosan Scaffolds for Bone Tissue Engineering: Structural Characterization and Evidence of Biocompatibility Features." Int. J. Polym. Sci., 2017, 2017, 8410750.

[9] Rufato, K., Galdino, J., Ody, K., Pereira, A., Corradini, E., Martins, A., Paulino, A., Fajardo, A., Aouada, F., Porta, F., Rubira, A. and Muniz, E., Hydrogels Based on Chitosan and Chitosan Derivatives for Biomedical Applications, Hydrogels - Smart Materials for Biomedical Applications, ed. L. Popa, London, United Kingdom, 2018. 1-40.

[10] Rachtanapun, P., Klunklin, W., Jantrawut, P., Jantanasakulwong, K., Phimolsiripol, Y., Seesuriyachan, P., Leksawasdi, N., Chaiyaso, T., Ruksiriwanich, W., Phongthai, S., Sommano, S. R., Punyodom, W., Reungsang, A. and Ngo, T. M. P., "Characterization of Chitosan Film Incorporated with Curcumin Extract." Polymers, 2021, 13, 963.

[11] Croisier, F. and Jérôme, C., "Chitosan-Based Biomaterials for Tissue Engineering." Eur. Polym. J., 2013, 49, 780-792.

[12] Muzzarelli, R. A. A., "Genipin-Crosslinked Chitosan Hydrogels as Biomedical and Pharmaceutical Aids." Carbohydr. Polym., 2009, 77, 1-9.

[13] Nozari, M., Gholizadeh, M., Zahiri Oghani, F. and Tahvildari, K., "Studies on Novel Chitosan/Alginate and Chitosan/Bentonite Flexible Films Incorporated with Zno Nano Particles for Accelerating Dermal Burn Healing: In Vivo and in Vitro Evaluation." Int. J. Biol. Macromol., 2021, 184, 235-249.

[14] Yadollahi, M., Gholamali, I., Namazi, H. and Aghazadeh, M., "Synthesis and Characterization of Antibacterial Carboxymethyl Cellulose/Zno Nanocomposite Hydrogels." Int. J. Biol. Macromol., 2015, 74, 136-141.

[15] Mishra, P., Mishra, H., Ekielski, A., Talegaonkar, S. and Vaidya, B., "Zinc Oxide Nanoparticles: A Promising Nanomaterial for Biomedical Applications." Drug Discov. Today, 2017, 22, 1-15.

[16] Devi, N. and Dutta, J., "Development and in Vitro Characterization of Chitosan/Starch/Halloysite Nanotubes Ternary Nanocomposite Films." Int. J. Biol. Macromol., 2019, 127, 222-231.

[17] Chen, M., Li, L., Xia, L., Jiang, S., Kong, Y., Chen, X. and Wang, H., "The Kinetics and Release Behaviour of Curcumin Loaded Ph-Responsive Plga/Chitosan Fibers with Antitumor Activity against Ht-29 Cells." Carbohydr. Polym., 2021, 265, 118077.

[18] Nyankson, E., Aboagye, S. O., Efavi, J. K., Agyei-Tuffour, B., Paemka, L., Asimeng, B. O., Balapangu, S., Arthur, P. K. and Tiburu, E. K., "Chitosan-Coated Halloysite Nanotubes as Vehicle for Controlled Drug Delivery to Mcf-7 Cancer Cells in Vitro." Materials (Basel), 2021, 14.

[19] Ang, L. F., Darwis, Y., Por, L. Y. and Yam, M. F., "Microencapsulation Curcuminoids for Effective Delivery in Pharmaceutical Application." Pharmaceutics, 2019, 11, 1-23.

[20] de Oliveira, A. C., de Lima, G. R. F., Klein, R. S., Souza, P. R., Vilsinski, B. H., Garcia, F. P., Nakamura, C. V. and Martins, A. F., "Thermo-and Ph-Responsive Chitosan/Gellan Gum Hydrogels Incorporated with the B-Cyclodextrin/Curcumin Inclusion Complex for Efficient Curcumin Delivery." React. Funct. Polym., 2021, 165, 104955.

[21] Varghese, J. S., Chellappa, N. and Fathima, N. N., "Gelatin–Carrageenan Hydrogels: Role of Pore Size Distribution on Drug Delivery Process." Colloids Surf. B. Biointerfaces, 2014, 113, 346-351.

[22] Karimi, A. R., Rostaminejad, B., Rahimi, L., Khodadadi, A., Khanmohammadi, H. and Shahriari, A., "Chitosan Hydrogels Cross-Linked with Tris(2-(2-

[DOI: 10.22068/ijmse.2633]

Formylphenoxy)Ethyl)Amine: Swelling and Drug Delivery." Int. J. Biol. Macromol., 2018, 118, 1863-1870.

[23] Ghaee, A., Bagheri-Khoulenjani, S., Amir Afshar, H. and Bogheiri, H., "Biomimetic Nanocomposite Scaffolds Based on Surface Modified Pcl-Nanofibers Containing Curcumin Embedded in Chitosan/Gelatin for Skin Regeneration." Compos. Part B: Eng., 2019, 177, 107339.

[24] Main Mechanisms to Control the Drug Release, in Strategies to Modify the Drug Release from Pharmaceutical Systems, Strategies to Modify the Drug Release from Pharmaceutical Systems, ed. Bruschi, M. L., 2015, Woodhead Publishing, United Kingdom, p. 37-62.

[25] Nguyen, V. C., Nguyen, V. B. and Hsieh, M.-F., "Curcumin - Loaded Chitosan / Gelatin Composite Sponge for Wound Healing Application." Int. J. Polym. Sci., 2013, 2013, 1-7.

[26] Hu, B., Gao, M., Boakye-Yiadom, K. O., Ho, W., Yu, W., Xu, X. and Zhang, X. Q., "An Intrinsically Bioactive Hydrogel with on-Demand Drug Release Behaviors for Diabetic Wound Healing." Bioact Mater, 2021, 6, 4592-4606.

[DOI: 10.22068/ijmse.2633]